URSI GASS 2020, Rome, Italy, 29 August - 5 September 2020

A Compact and Lightweight Ultra-Wideband Interferometer for Direction Finding Applications

L. Scorrano[(1)], A. Calcaterra[(1)], P. Bia[(1)],
S. Maddio[(2)] and G. Pelosi[(2)], M. Righini[(2)], S. Selleri[(2)]
(1) Elettronica S.p.A., Roma, Italy,
(2) DINFO - University of Florence, Florence, Italy

Abstract

In this work it is proposed the design of a couple of UWB two-arm sinuous antennas working in 2-18 GHz (Antenna A) and 6-18 GHz (Antenna B) frequency bands assembled in a ultra-wideband array for direction finding applications. Both antennas work with a slant 45° polarization ensuring good matching impedance and stable radiation characteristics in the considered frequency bands. The design has been optimized in order to reduce the geometrical dimensions. The proposed antennas have been manufactured and tested in order to validate the simulation performances. Finally the evaluation of accuracy performances in estimating the direction of arrival of an incoming wave-front is presented.

1 Introduction

The sinuous antenna is a very appealing and versatile ultra-wideband (UWB) antenna. Originally introduced and patented by Du Hamel in 1987 [1], it has been used both in its dipole and slot versions, both with two or four arms [2–6].

In particular, two-arm dipole sinuous antennas are very interesting for homeland security applications. Their UWB characteristic and linear polarization allow the design of interesting systems for passive detection of targets. Effective radio-goniometers can be devised by employing a limited number of sinuous antennas in slant 45° polarization. UWB and slant polarization allows to effectively detect any incoming signal generated by the targets.

In this contribution the design of two sinuous antennas, one covering the 2-18GHz band and one covering the 6-18GHz band is presented. Stringent constraints on overall size are given to be able to pack the antenna tightly enough to build an effective radio-goniometer. An overview of the backing lossy-loaded cavity and balun, necessary for single mode operation, will also be given.

2 Antenna design

The sinuous antenna layout is reported in Fig. 1. The equation of the profile can easily be retrieved in literature [3-6] and will not be reported here for brevity. Key points are that lower working frequency is limited by the outer diameter of the antenna, while the upper frequency is limited by how close the feeding point can be manufactured.

The 6-18GHz, hereafter indicated as “Antenna A” diameter must be at maximum 20mm, while the 2-18GHz, hereafter indicated as “Antenna B” diameter must be at maximum 60mm, furthermore photolithographic process cannot create lines/slots thinner than about 100μm, limiting upper frequency. These dimensional requirements are very hard to comply. In particular the theoretical analytic profile has been modified so as to never produce lines thinner than 100μm in the feeding area.

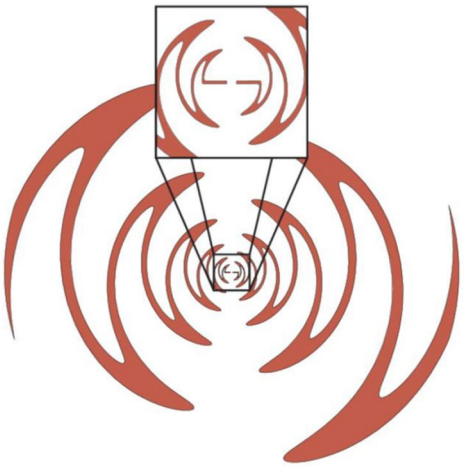

Figure 1. Two arm microstrip antenna layout. With zoom on the feeding point area.

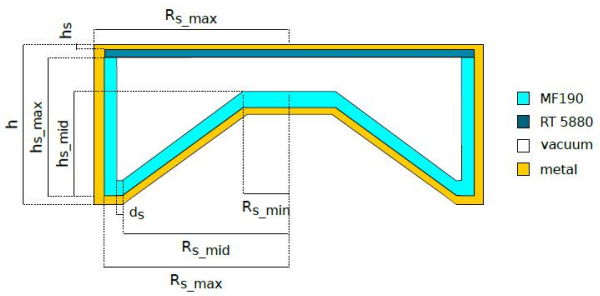

Figure 2. Side view of the antenna (top plate) backed by a shaped cavity loaded with lossy ECCOSORB-MF190.

These dimensional requirements were met by designing the antennas on a Rogers 5880 substrate, 0.245mm thick (ε_r = 2.2, tanδ in the range 0.0004 to 0.0009).
To obtain a single lobe pattern the antenna is backed with an ECCOSORB-MF190 absorber, with tanδ up to 4 in our frequency range.

A critical design feature is the balun, which, of course, must have at least the same bandwidth of the antenna. Two classes of baluns have been studied. A tapered Klopfenstein balun, to be mounted orthogonally to the antenna (Fig. 3) for the Antenna A. In the 6-18GHz band the tapered line balun is sufficiently small for the proposed application, but in the 2-18GHz it would be too bulky. Hence for the Antenna B a slot line balun (Fig. 4) [7] is proposed, to be mounted parallel to the antenna and connected via semi-flexible coaxial cable short segments. This latter balun is more compact than the tapered line one and allows for a lower profile for the larger antenna B.

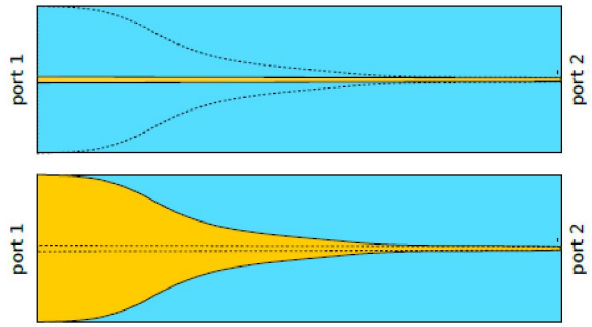

Figure 3. Tapered balun with impedance transformation from unbalanced 50Ω misrostrip (left) to balanced 100Ω double-sided parallel-strip line.

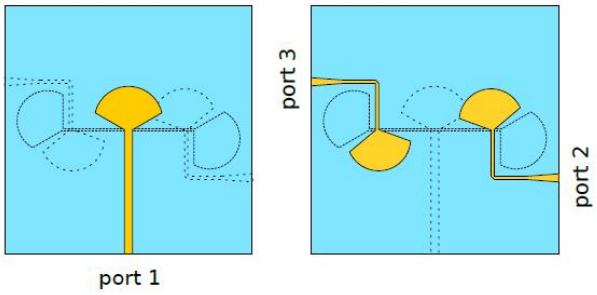

Figure 4. Slotline balun with wide band stubs and impedance transformation.

3 Simulations and measurements

The proposed antennas A and B have been simulated in frequency-domain with full-wave electromagnetic software CST Microwave Studio [8]. The obtained 3D radiation pattern of the Slant 45 (S45) polarization shows a high symmetry on the azimuth plane for both antennas in all the working frequency bands. In Fig. 5 it is illustrated a radiation pattern for antenna B, slant 45° (S45) polarization, at the frequency f = 12 GHz. The obtained radiation pattern characteristics exhibit a good symmetry on the azimuth plane with a boresight realized gain of the S45 polarization of 3.8 dBi and an half power beam width (HPBW) of 75°.

In Fig. 6 it is illustrated the radiation pattern S45 for the Antenna A at the frequency f = 6 GHz.

The obtained radiation pattern characteristics exhibit the same good symmetry on the azimuth plane with a boresight realized gain of the S45 polarization of 3.3 dBi and an half power beam width (HPBW) of 80°.

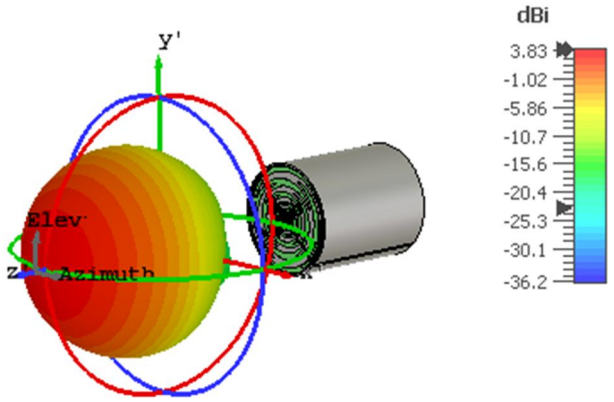

Figure 5 3D radiation pattern S45 of the Antenna B at frequency f = 12 GHz.

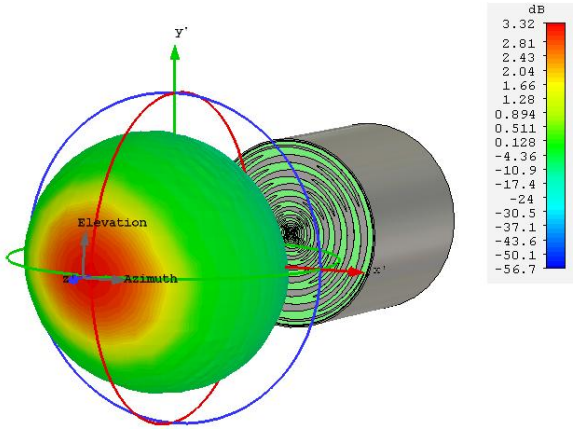

Figure 6 3D radiation pattern S45 of the Antenna A at frequency f = 6 GHz.

To validate the electromagnetic properties evaluated by numerical simulation, the prototype of such antennas have been realized and measured. The manufactured Antenna A and Antenna B are shown respectively onto the left and right in Fig. 7.

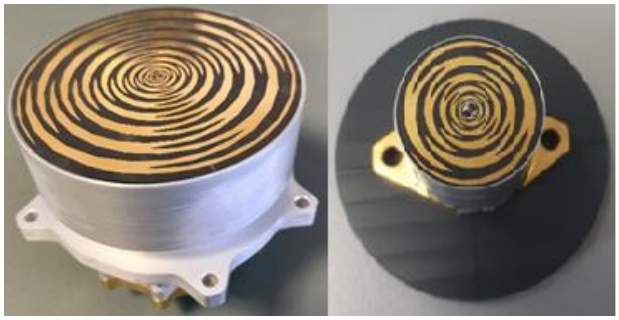

Figure 7 Manufactured antennas: Antenna A (left) and Antenna B (right).

The antenna prototypes has been characterized by using a On The Air Near Field to Far Field system (OTA NF-FF). The measured performances have been compared with the simulated ones. In particular, in Fig. 8 and Fig. 9 the S11 and the realized boresight gain S45 of the Antenna A are compared. The performance comparison shows a good agreement between simulated and measured performances. In fact, the Reflection coefficient presents a value below -5 dB all over the frequency bandwidth and the resonances are clear visible in both case. The realized gain measured presents the same behavior of the simulated one, the negligible differences are due to the difficult of modelling with high accuracy the absorber material present inside the cavity.

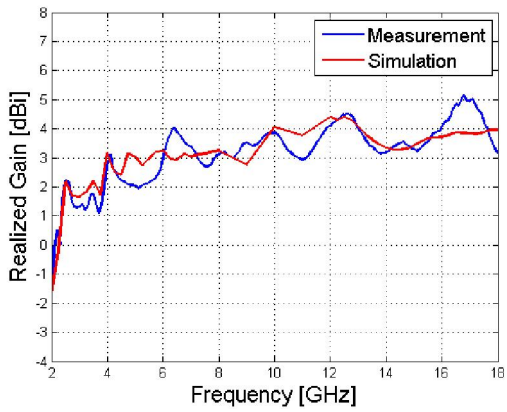

Figure 8 Comparison between measurement and simulation of the Realized Gain at Boresight for the Antenna A.

In Fig. 10 and Fig. 11 are compared the S11 and the realized boresight gain S45 of the Antenna B. Also for this antenna, the performance comparison between simulation and measurement are in good agreement both for the Reflection coefficient and the boresight realized gain.

4 Conclusion

This work described the design of two sinuous UWB antenna working in 2-18 GHz (Antenna A) and 6-18 GHz (Antenna B) frequency bands. Both antennas have been

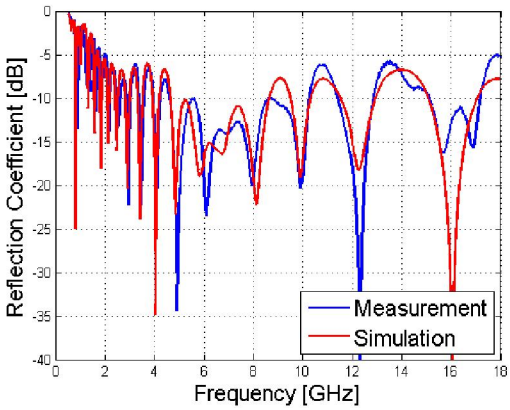

Figure 9 Comparison between measurement and simulation of the Reflection Coefficient for the Antenna A.

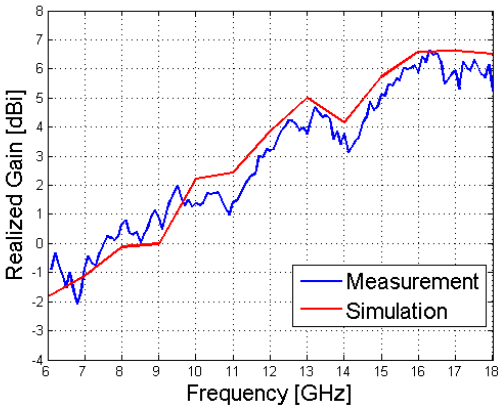

Figure 10 Comparison between measurement and simulation of the Realized Gain at Boresight for the Antenna B.

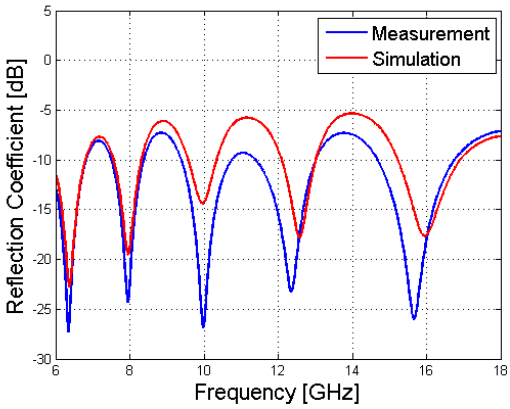

Figure 11 Comparison between measurement and simulation of the Reflection Coefficient for the Antenna B.

optimized to fulfill challenging dimensional requirements. The simulated performances have been validated by measurements by using a Near Field to Far Field system. The resulting performances in terms of accuracy of the direction of arrival estimate have been evaluated

considering a three-channel receiver, switching between a set of three antennas of type A and three antennas of type B, a signal-to-noise ratio equal to 20dB, and a correlative algorithm based on the measured results presented in Section 3. The synthetic results coming from Montecarlo simulations applied to the measured antenna patterns are shown in Fig. 12.

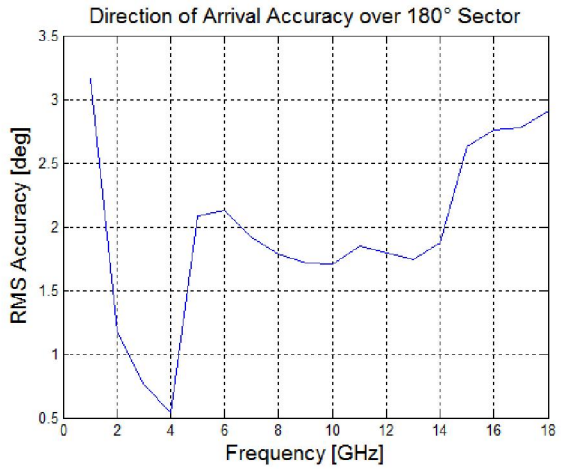

Figure 12 Direction of Arrival accuracy performance of the antennas depicted in Fig 7.

5 Acknowledgements

The authors wish to thank the people whose assistance, during the last two years, was a significant contribution in the completion of this project, as well as for their useful suggestions and interesting conversations that greatly enhanced the quality of this paper: R. Ardoino, M. Bartocci, A. Lunardi, A. Manna, G. Panci and A. Zaccaron.

6 References

1. R.H. DuHamel. “Dual polarized sinuous antennas,” *US Patent* 4,658,262. Apr. 1987.

2. Elettronica S.p.A. “Ultra-wide-band low-profile sinuous slot antenna array,” *EP Patent* 2,629,367,B1. 2016.

3. S. Lizhong, C. Guojin, H. Huanfeng, “Simulation and analysis of a hemispherical conformal sinuous antenna with four arms,” *Proc. IEEE Int. Conf. Ultra-Wideband (ICUWB)*, 2010, vol. 1, pp. 1–4.

4. A. Manna, P. Baldonero, F. Trotta, “Novel UWB lowprofile sinuous slot antenna,” *Proc. 5th Eur. Conf. Antennas Propag. (EUCAP)*, 2011, pp. 783–786.

5. E. Agastra, L. Lucci, G. Pelosi, S. Selleri, “High gain compact strip and slot UWB sinuous antennas,” *Int. J. Antennas Propag.* , vol. 2012, 9 pp., 2012.

6. L. Bartalucci, S. Maddio, G. Pelosi, M. Righini, L. Scorrano, S. Selleri, “A ultra wide band sinuous antenna design with enhanced linear polarization purity,” *in 2019 URSI Asia-Pacific Radio Science Conference (AP-RASC)*, New Delhi (India), 09-15 March 2019, pp. 1–2.

7. A. K. Poddar, U. L. Rohde, V. Madhavan and S. K. Koul, "A novel UWB Balun: Application in 5G systems," in *2016 IEEE International Frequency Control Symposium (IFCS)*, New Orleans, LA, 2016, pp. 1-7.

8. CST Microwave Studio, CST Computer Simulation Technology AG.